RSC Advances

ROYAL SOCIETY OF CHEMISTRY

www.rsc.org/advances

RSC Advances

RSCPublishing

ARTICLE

Fluorescence detection of the pathogenic bacteria *Vibrio harveyi* in solutions and animal cells using semiconductor quantum dots

Cite this: DOI: 10.1039/x0xx00000x

Received 00th September 2015,
Accepted 00th xxxx 2016

DOI: 10.1039/x0xx00000x

www.rsc.org/

Esha Arshad,[1] Abdulaziz Anas,[2,*] Aparna Asok,[1] C. Jasmin,[2] Somnath S. Pai,[3] I. S. Bright Singh,[1] A. Mohandas,[1] Vasudevanpillai Biju[4,*]

Validation of microbial infection pathways in Eukaryotic cells is challenging in the control of various infectious diseases. Semiconductor nanocrystals, also called quantum dots (QD), due to their exceptional brightness and photostability can be exploited in the long term monitoring of pathogens in host cells. However, the limited information about interactions of QDs and their bioconjugates with microorganisms confines the microbiological applications of QDs. Here we investigate the binding and toxicity of CdSe/ZnS QDs to the free-swimming marine pathogenic bacteria *Vibrio harveyi* using fluorescence microscopy, elastase assay, polyacrylamide gel electrophoresis (PAGE), and comet assay. The electrostatic binding of QDs to the cell surface has been found effective for the detection of the bacteria in aqueous solutions and bacteria-infected mammalian cells. The electrostatic binding is evaluated by the transient reversal of the cell surface charge contributed by macromolecules such as heparan sulfate proteoglycan (HSPG). Essentially, no fluorescence is detected for those bacteria treated with $NiCl_2$ that reverses the cell surface charge. On the other hand, the efficiency of the cell surface to adsorb QDs remains intact even after the treatment with elastase, which denatures the outer membrane proteins (Omps), suggesting HSPG-based binding of QD to cell surface and subsequently QDs are internalized. PAGE and comet assays show that the interactions of QDs with *V. harveyi* do not impart any cytotoxicity or genotoxicity. Further, we evaluate the integrity of adsorbed QDs for the detection of bacterial infection to mammalian cells by taking mouse fibroblast L929 as the model. Here, the stable fluorescence of QDs present in *V. harveyi* enables us for identifying the infected host cells. In short, the current study shows the potentials of QDs for the detection of pathogens but without causing any toxic effects, which when combined with the stable fluorescence of QDs can be a promising method for not only the detection of the progression or regression of pathogenic infections but also phototherapy of microbial infections.

1. Introduction

Bioconjugated quantum dots (QDs) have become fundamental parts of *in vitro* and *in vivo* imaging of cells, subcellular structures, and vital biomolecular functioning.[1-3] Owing to the exceptional photostability and brightness of QDs, their conjugates with biomolecules such as antibodies,[4] peptides,[5] hormones,[6] nucleic acids,[7] small organic and bioorganic molecules,[8] and liposomes[9] have been extensively evaluated in bioimaging. In particular, bioconjugated QDs effectively replace organic dye molecules in live cell imaging when photostability and multiplexing are needed. For example, conjugates of QDs with specific tags enable us for the efficient detection of extracellular receptors,[10] intracellular cargo transport,[5, 9] gene and drug delivery,[11, 12] cell membrane dynamics,[10] and cancer cells.[6] Advantages of QDs over organic dyes for bioimaging are discussed in recent review articles.[3, 13] Lately, bioconjugated QDs are infiltrating into areas such as microarray detection of proteins[14] and infectious diseases.[15, 16] More importantly, on the basis of recent investigations of photosensitized generation of reactive oxygen and nitrogen intermediates by QDs, potential of QDs for photodynamic therapy has been recognized.[17, 18] Despite such infiltration of QDs technology into biology, an interface between microbiology and QDs is yet to be established, which may lead to the detection of pathogens, monitoring of the progression or regression of infectious diseases, and phototherapy of microbial infections in human or animal models.

Although several groups of bacteria are beneficial to human or animal health as probiotics or key players in biogeochemical cycles and sources of bioactive compounds or industrially important enzymes, some are pathogens. Recently, an interface between nanotechnology and microbiology has emerged, for which nanoparticles-based barcodes for the detection of bacterial pathogens and bacteria-based intracellular delivery of nanoparticles are the bases.[19, 20] The application of QDs in microbiology was first realized by Kloepfer and co-workers in 2003[19] by evaluating the use of CdSe QDs conjugated with wheat germ agglutinin and transferrin protein for the strain- and metabolism-specific microbial labelling of bacterial and fungal pathogens. Later, Zhu and co-workers reported an antibody probe for the immunofluorescence detection of two waterborne pathogens, Cryptosporidium and Giardia.[16] Yet another example is the development of a novel protocol for the simultaneous enrichment and the detection of three food-borne bacterial strains, *Salmonella typhimurium*, *Shigella flexneri* and *Escherichia coli*, using antibody-conjugated QDs and magnetic nanoparticles.[15] Tracking of the infection pathway of microorganisms in animal models can be an attractive application of QDs as they facilitate *in vivo* imaging several millimetres under the skin owing to their NIR photoluminescence (PL), high-PL quantum yields, broadband

absorption of light extending in the UV-Vis-NIR regions, large Stokes-shift, exceptional photostability, and large cross-section for one and two-photon absorbencies.[21, 22] Despite the development of non-toxic QDs such as silicon and carbon, a bridging gap exists between QDs and their applications in both tracking of infection pathways in animal models and therapy against infections, which is the limited information about interactions of QDs with microbial cell membrane and toxicity of QDs to microorganisms.

Recently, Priester and co-workers studied the effects of soluble cadmium salts and CdSe QDs on the growth of planktonic *Pseudomonas aeruginosa* and detected impairment of bacterial growth,[23] which is attributed to the cytotoxic effects of cadmium ions released from CdSe QDs. Such toxic effect of core-only CdSe QDs to mammalian cells is widely known. Thus, protection of the core with shells from polymers, silica, ZnS, etc. has been extensively investigated.[13, 21] Mahendra and co-workers [24] have shown that QDs with intact surface coatings cannot show bactericidal properties. Nonetheless, the binding mode of QD to pathogens, stability of QDs and toxicity to pathogen are central issues to be resolved in the microbiological applications of QDs. Here, we report the charge-based interactions of CdSe/ZnS QDs with the marine pathogen *Vibrio harveyi* (*V. harveyi*) and toxic effects of QDs to bacterial cells, and demonstrate tracking of bacterial infection to animal cells. We used techniques such as fluorescence microscopy, elastase assay, PAGE, and comet assay to evaluate the interactions of QDs with *V. harveyi* and the subsequent effects of QDs on the integrity of the bacterial cell membrane and stability of genetic materials. Our studies show that irreversible charge-based interactions of QDs with lipopolysaccharides (LPS) and proteoglycans can be utilized for the labelling of microorganisms. Also, the current study shows that QDs neither alter the integrity of the cell wall nor impair the DNA of *V. harveyi*. Thus, QDs are ideal labels for the detection of pathogens and the progression or regression of pathogenic infections.

2. Results and Discussion

To investigate the roles of Omps and cell surface charge on the binding of QDs to *V. harveyi*, the integrity of the cell membrane, and the stability of genetic material, we have applied different concentrations of QDs (1 pM to 1 nM) to live *V. harveyi*. Here, QDs efficiently attach to the cells, which is evident from the bright yellow fluorescence of the cells (Figure 1A). Interestingly, the fluorescence intensity of the cells remained intact even after repeated washing using PBS, which suggests irreversible binding of QDs to the cell membrane. The cells labelled using QDs provide 100-fold bright PL signal when compared with the fluorescence of cells labelled using streptavidin conjugated FITC.[25] Besides, the fluorescence spectrum of QDs remained intact even after binding to the cells (Figure 1B). The stable binding of QDs to the bacterial cell membrane makes it possible for us to visualize individual bacteria for an extended period of time, which is analogous to the detection of *E. coli* single cells using QDs by Hahn *et al*.[25] Nonetheless, the origin of irreversible binding of QDs to microorganisms remain unsolved, leaving us with two possibilities: binding of streptavidin on QDs to Omps and electrostatic interactions.

It is known that Omps on the surface of bacteria show natural affinity for streptavidin.[26] To evaluate whether or not interactions of Omps with streptavidin play a major role on the biding of QDs to the cell membrane, we saturated a *V. harveyi* sample with free streptavidin, and subsequently the cells were treated with QDs and examined the fluorescence of the cells. Figure 2A shows the fluorescence image of *V. harveyi* first saturated with free streptavidin

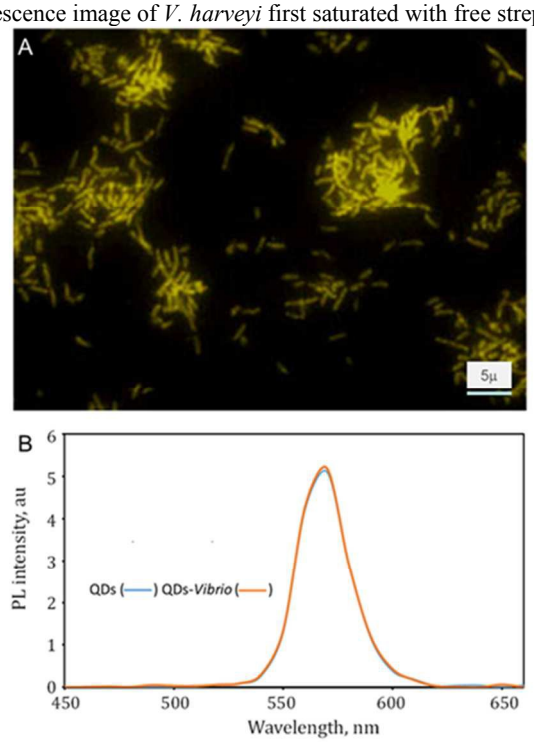

Fig 1. (A) Fluorescence image of *V. harveyi* cells in a bacteria sample treated with CdSe/ZnS QDs (2 pM). (B) Fluorescence spectra of QDs without and after tethering to *V. harveyi*.

and then incubated with a solution of QDs (2 pM). The fluorescence intensities of the cells were essentially comparable to that of cells without any streptavidin pre-treatment. In other words, the pre-saturation of Omps in *V. harveyi* with streptavidin does not suppress the efficiency of QDs to bind with the cell membrane, suggesting that Omps-streptavidin interactions do not play any significant role on the binding of QDs to *V. harveyi*. To further confirm the role of Omps on the QD labelling process, we next pre-incubated *V. harveyi* with elastase before the addition of QDs.[27] Here elastase is selected for its ability to change the conformation of Omps and denature them. Nevertheless, the QD labelling efficiency of cells treated with elastase remained essentially the same as that of untreated fells (Figure 2B).

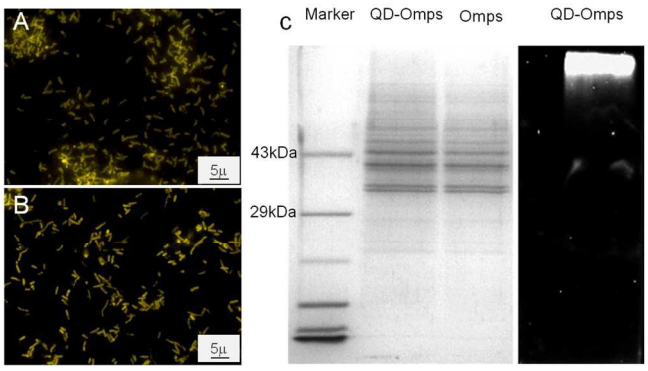

Fig 2. Fluorescence images of *V. harveyi* incubated with CdSe/ZnS QDs under various conditions: (A) *V. harveyi* were pre-saturated with streptavidin or (B) 1U elastase enzyme (B) before incubation with QDs. (C) SDS PAGE image of QD-Omps conjugate

under white light (left) and UV illumination (right). QDs are not conjugated with Omps and do not move with Omps as seen in the PAGE bands.

These observations suggest that Omps are not involved in the binding of QDs to *V. harveyi*. The role of Omps on the binding of QDs to the cell membrane was further evaluated by the poly acrylamide gel electrophoresis (PAGE) of purified Omps and QD-Omp conjugates (Figure 2C). Immediately after the electrophoresis, the gel was transferred into a gel documentation system and illuminated with white or UV light. The white light excitation indicated three bands between 29 and 43kDa, and a few bands beyond 43kDa, which are typical for Omps.[28] Importantly, the fluorescence of QDs was detected at the extreme top of the gel, which is different from fluorescence bands of Omps (Figure 2C). These observations conform that the binding of QDs to *V. harveyi* is independent of non-specific interactions to Opms.

To understand the role of cell surface charge, which is contributed by heparin sulfate proteoglycans (HSPG), lipopolysaccharides (LPS) and other negatively charged moieties, on the binding of QDs to *V. harveyi*, we next designed and carried out an experiment to reverse the surface charge of *V. harveyi*. The slow migration pattern of QDs (lane 2) in agarose gel compared to that of DNA ladder (lane 1) and control plasmid (lane 3) indicate their net positive charge (Figure 3A). When an electric field is applied, DNA moves towards the anode in an agarose gel electrophoresis due to their negative charge and segregate into different bands based on their molecular weight, while the net positive charge of QDs retards their migrations towards anode. The streptavidin conjugated CdSe/ZnS QDs have Zeta potential value ca -0.15 mV, which confirms their net positive charge.[29] The cell surface of bacteria due to the presence of HSPG, LPS and other phosphate/sulphate groups carry net negative charge,[30] which permits electrostatic interactions with positively charged QDs (Figure 3B). Here, the interactions of positively charged QDs to *V. harveyi* before and after treatment with $NiCl_2$ were investigated using fluorescence

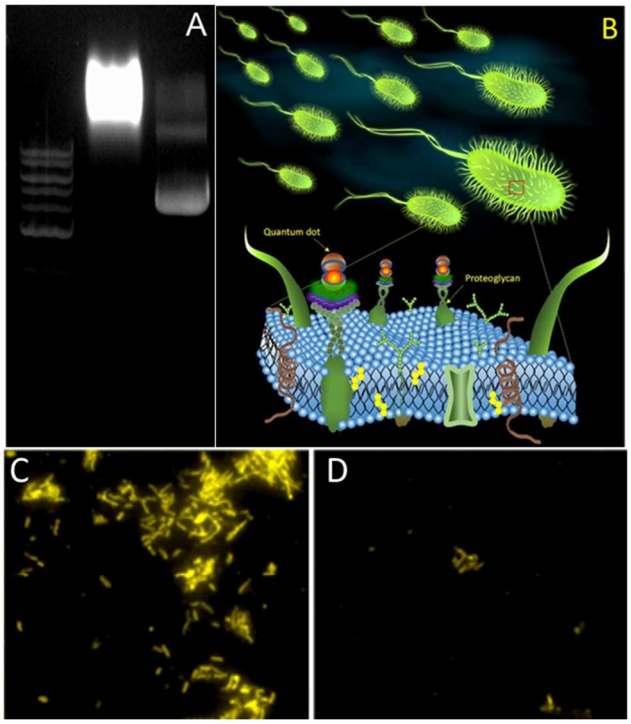

Fig 3. (A) Agarose gel image of 1kb DNA marker (left lane), CdSe/ZnS QDs (central lave) and plasmid DNA (right lane) (pUC18) stained with SYBR. (B) Schematic presentation of the binding of CdSe/ZnS QDs to *V. harveyi*. (C, D) Fluorescence images of *V. harveyi* treated with CdSe/ZnS QDs (C) before and (D) after reversal of the cell surface charge using Ni^{2+}.

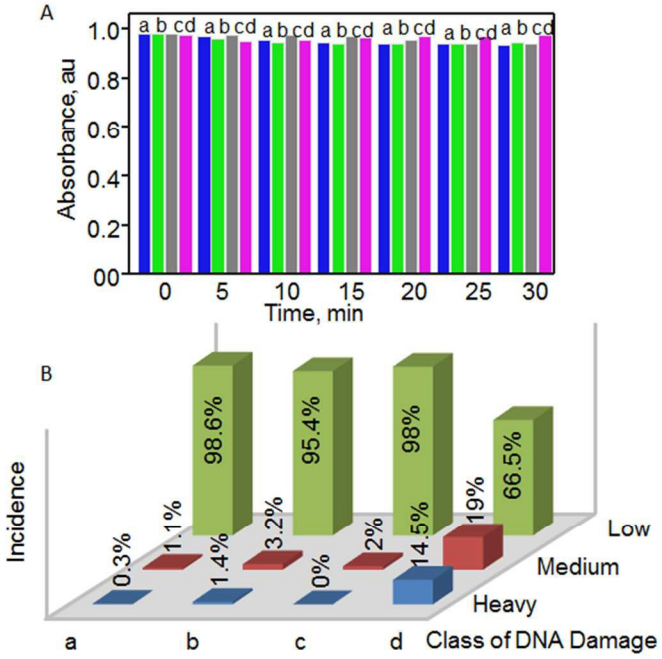

Fig 4. (A) Histogram showing SDS assay of the cell membrane integrity of *V. harveyi* (a) before and (b) after treatment with $CdCl_2$, and (c) with and (d) without photoactivation in the presence of CdSe/ZnS QDs. (B) Histogram of comet assay of *V. harveyi*: (a) *V. harveyi* alone, (b,c) *V. harveyi* treated with 2 pM CdSe/ZnS QDs- (b) before and (c) after exposure to light, and (d) *V. harveyi* treated with $CdCl_2$. Comets are classified based on tail length into Low (0-10 mm), Medium (10-20 mm) and Heavy (20-30 mm) damage groups.

microscopy. We reversed the cell surface charge by a short exposure of *V. harveyi* to $NiCl_2$ at a pH of 8.5, which was carried out by following a method reported in the literature.[31] Interestingly, Ni^{2+} hindered the interactions of QDs with the cell surface (Figure 3C), suggesting that reversal of the cell surface charge as a result of the interactions of divalent Ni ions with the negatively charged cell surface moieties significantly suppress the density of QDs on the cell membrane. In other words, charge-based interactions between QDs and cell surface play a pivotal role on the labelling mechanism (Figure 3D). Nevertheless, stable fluorescence bacterial cells without any $NiCl_2$ pre-treatment suggests a possibility of binding of QDs to HSPG and subsequently, the bound QDs are internalized by HSPG. The application of positively charged QDs and other nanoparticles for effective labeling of animal cells such as neuronal and tumour cells are reported.[29, 32, 33] In such studies, QDs with different functional groups like carboxyl, amino-PEG and streptavidin were used. Here, we selected streptavidin functionalized QD by considering its wide acceptance in biotin-based labeling of biomolecules for both *in vitro* and *in vivo* applications.

We next investigated whether or not charge-based labelling of QDs to the surface of *V. harveyi* induce any toxic effects to the integrity of the cell membrane or the genetic materials, which was carried out by optical measurements of bacterial samples treated with QDs. Here, *V. harveyi* were cultured overnight at room temperature and washed copiously with PBS.

The bacteria were then transferred into sterile cuvettes and treated with QDs (1 nM) or $CdCl_2$ (500 µM) and 0.1 % aqueous SDS solution. The integrity of the cell membrane was evaluated from the optical density recorded at every 5 min with or without photoactivation. Figure 4A shows the SDS assay for the bacterial samples treated with QDs or $CdCl_2$ under different conditions. The optical density at 600 nm (A600) remained essentially intact, suggesting that QDs electrostatically attached to the cell surface do not affect the integrity of the cell membrane. On the other hand, bacteria with disintegrated cell membrane easily undergo SDS-mediated cell lysis and as a result, a sharp drop in the optical density (A600) is expected.[26] Such SDS-mediated lysis occurs to cell because the detergent intensifies the damage to the membrane and causes the cell contents to leak out, which is widely known. Here the constant optical density of *V. harveyi* treated under normal or photo-excited conditions with QDs suggests the nontoxic nature of QDs tethered to the cell surface.

To investigate the toxicity of QDs to the genetic material of *V. harveyi*, we employed comet assay, which is a standard method for *in vitro* and *in vivo* monitoring of the genotoxicity of both eukaryotic and prokaryotic cells.[34] In comet assay, DNA fragments resulting from the single strand or double strand breakage in cells embedded in the agarose gel migrate faster in the electric field than intact DNA. The comets (500 numbers) formed as a result of electrophoresis were imaged using a fluorescence microscope and the damage to DNA was classified on the basis of the length of the comets (Figure 4B). The fluorescence intensity of the comet tail is directly related to the frequency of DNA breakage, which are assessed using densitometry followed by computer-aided analysis. The comets are ranked into low (0–10 µm) medium (10–20 µm) and high (>20 µm) damaged ones on the basis of the lengths of comet tail. In the current work, the genetic materials of over 95 % *V. harveyi* cells remained intact even after treatment with QDs with or without photo-activation, which suggests that QDs do not directly interact with the DNA of bacteria. On the other hand, we detected damage and breakage of plasmid DNA directly labeled with QDs and photo-activated. However, the DNA damage was significant when *V. harveyi* were exposed to $CdCl_2$ alone, which also suggests that the amount of cadmium ion released is not significant for commercial QDs. Also we observed no significant difference in the growth rate of *V. harveyi,* before and after exposure to CdSe/ZnS QDs. As seen in Fig. 5, *V. harveyi* cells before and after exposure to QDs show a growth rate of 2.15 ± 0.05 and 1.97 ± 0.04 h^{-1} respectively. On the other hand, cells exposed to a solution of $CdCl_2$ show negative growth rate of – 0.143 ± 0.04 h^{-1} (Fig. 5). These observations suggest commercial streptavidin-conjugated QDs are non-toxic under the selected experimental conditions. Nonetheless, CdSe-based QDs are known to release Cd^{2+} ions under various conditions, which include enzymatic reactions in cell microenvironments[35] and prolonged exposure in the solution phase to high intensity laser light.[36,37]

The toxicity of QDs due to the release of Cd^{2+} ions and the subsequent generation of free radicals is recognized in cell-based assays. For example, the excessive release of Cd^{2+} ions from mercaptoacetic acid capped CdSe QDs inhibits the growth of mammalian cells[38] and bacterial pathogens such as *E. coli* and *Staphylococcus aureus*.[39] The toxicity induced as a result of the release of Cd^{2+} ions could be largely suppressed by the coating of QD with different shell materials such as silica and polymers.[21] Previously, Ipe *et al*. evaluated the release of Cd^{2+} from QDs by measuring the photoinduced generation of free radicals of 5,5-dimethyl-1-pyrroline N-oxide in the presence of CdSe and CdSe/ZnS QDs.[40] Interestingly, the release of Cd^{2+} and the generation of free radicals was completely suppressed in the case of ZnS shelled CdSe QDs.[40] Despite these reports on the release of Cd^{2+} from cadmium chalcogenide QDs and the related toxicity to human, animal and bacterial cells, the exact mechanism underlying the interactions of QDs to cell membrane remain unsolved. We find that commercial QDs strongly bind to bacterial cell surface through electrostatic interaction, but without

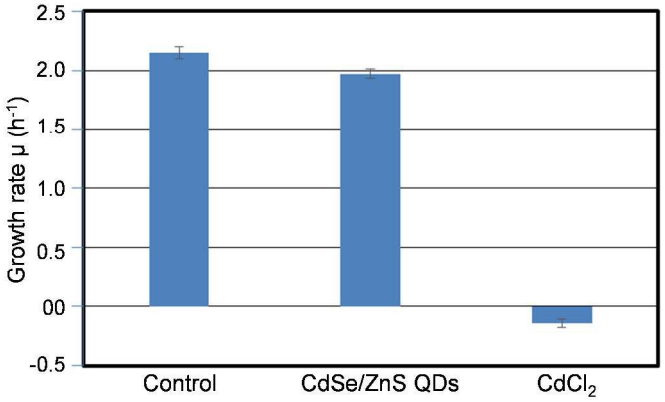

Fig 5. Histogram of growth rate of *V. harveyi* exposed to QDs (1 nM). Cells without any QDs or treated with a $CdCl_2$ solution (500 uM) are controls.

involving non-specific binding to Omps or inducing any toxicity. Non-toxic nature of QDs is assigned to their inability to cross the cell membrane. Here, passive internalization of QDs is unviable in bacterial cells, because the hydrodynamic size of QDs involved (ca 15 nm) is larger than the biggest globular protein that passes through the intact bacterial cell membrane. Also, the largest pores, known as permeases for excreting proteins from bacteria, open to a maximum of 6 nm in diameter.[41] Nevertheless, QDs with specific surface modification are delivered by pathway-dependent mechanisms. For example, adenine-conjugated QDs (size <5 nm) are efficiently taken up in Bacillus subtilis by purine-dependent transport.[42]

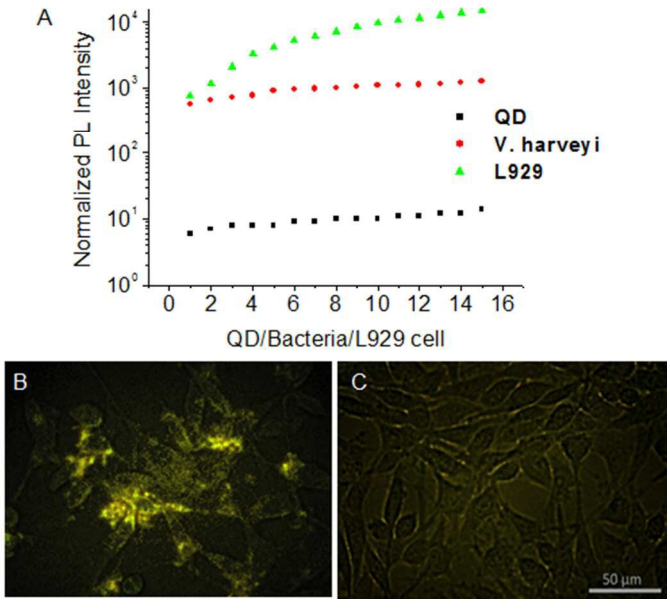

Fig 6. (A) Photoluminescence intensity histograms of QDs, *V. harveyi* and L929 cells arranged in the ascending intensity order. The intensity values are obtained on the basis of pixel/intensity for single QD sample, QD-*V. harveyi* conjugate sample, and L929

sample. The intensity values suggest on average 90 QDs/bacteria and 1-12 bacterial infection/L929 cells. (B, C) Overlay of phase and fluorescence images of L929 cells incubated with (B) QD-*V. harveyi* conjugate and (C) QDs alone. The fluorescence of QD-bacteria conjugate in B confirms infection to L929 cells.

The efficient binding of QDs to bacterial cell surface, but without causing any toxicity, may find application such as tracking of bacterial infections and intracellular delivery of theranostics. To test the potentials of QD-labeled bacteria for the detection of bacterial infection to mammalian cells, we treated mouse C3H/An connective tissue cell **(**L929 cells) with QD-labeled *V. harveyi* and examined the fluorescence of bacteria present in L929 cells. To validate the infection of L929 cells by *V. harveyi*, fluorescence intensities of single QDs are compared with that of bacteria and L929 cells (Figure 6A). Here the intensity of bacteria is two orders of magnitude higher than that of single QDs, which suggests an average of 100 QDs/*V harveyi*. When compared with single QDs, the fluorescence intensity of L929 is 2 to 3 orders of magnitude, indicating 1 to 10 bacterial infections per cells. Figure 6A shows fluorescence intensity of single QDs Figure 6B shows the overlay of phase and fluorescence image of L929 cells incubated with QD-bacteria conjugates. Here, the intracellular fluorescence of QD-bacteria conjugate indicates infection of L929 cells. On the other hand, L929 cells treated with QD alone (Figure 6C) do not show any intracellular fluorescence. In other words, *V. harveyi* acts as an intracellular delivery vehicle of QDs. Further, this preliminary test indicates the potentials of QD-bacteria conjugates for the prolonged monitoring of pathogenic infections to mammalian cells. A similar strategy was reported by White *et al*.[43] by the fluorescence detection of anionic phospholipids of bacteria as a model system of bacterial infection in living mice. The principle of fluorescence labelling and detection of infection in this case is the charge-based interaction of bis (Zn-PDA) ligands of a deep-red fluorescent squaraine rotaxane dye with anionic phospholipids of bacteria. Other reports in this line are the use of cholerae toxinB for intracellular delivery of QDs in mammalian cells,[44] and bacteria micro-boat for the intracellular delivery of nanoparticles in animal cells and solid tumour.[20] In other words, with the simple and stable binding of QDs to *V. harveyi* and the delivery of QD-*V. harveyi* assembly in L929 cells, we show direct detection of bacterial infection to mammalian cells. Such bacteria based fluorescence imaging of mammalian cells is expected to advance both nanoparticle-based detection of pathogenic infections and delivery of theranostics.

3. Conclusions

Our investigations show that CdSe/ZnS QDs are cytotoxically and genetically safe label for bacteria allowing for live imaging of microorganisms at single cell resolution and also for tracking of microbial infection cycle in animal cells. Here the electrostatic binding of QDs to the cell surface is the basis of the detection of *V. harveyi* in aqueous solutions and in connective tissue cells. The binding of QDs to *V. harveyi* is facilitated by electrostatic interaction with negatively charged moieties such as HSPG and LPS in the cell membrane, which is evidenced by the reversal of cell surface charge; whereas the Omps do not interact with QDs, which was determined by treatment of *V. harveyi* with elastase and the subsequent PAGE assay. Thus, the stable binding of QDs to the cell membrane when combined with the bright and stable emission and broad absorption and narrow emission bands of QDs not only becomes attractive for multiplexed imaging of pathogens or probiotics life cycle of bacteria but also facilitate simple charge-based microbial assemblies for intracellular delivery of cargos.

4. Experimental Section

4.1. Bacterial culture and labeling

V. harveyi (MCCB 111) was obtained from the culture collection of National Centre for Aquatic Animal Health (NCAAH), Cochin University of Science and Technology, India. *V. harveyi* sample was inoculated into ZoBell's marine broth prepared in 15 ppt seawater and grown overnight at 28 ± 2 °C on a shaker incubator at 120 rpm. Working cultures of *V. harveyi* were maintained on ZoBell's marine agar slants and subcultured every 2-3 weeks. The purity of the culture was confirmed by Gram staining and fatty acid profiling.

Overnight cultures of *V. harveyi* were washed and re-suspended in phosphate buffered saline (PBS; 8 g NaCl, 0.2 g KCl and 1.44 g KH2PO4 prepared in 1L distilled water, pH 7.4) to a final concentration of 10^6 cells mL^{-1}. The cells were incubated separately with 1 pM, 2 pM and 1 nM solutions of streptavidin-functionalized CdSe/ZnS quantum dots for 30 min. The emission spectra of QDs and QDs-bacteria samples were measured in a multimode microplate reader (Biotek USA). Samples for studying the role of streptavidin and Omps on QD-bacteria interactions were prepared by pre-incubation of the *V. harveyi* cells with solutions of streptavidin or 1 U of esterase enzyme, which was followed by treatment with 1 nM solutions of CdSe/ZnS QDs. Similarly, the samples for studying the effect of cell surface charge on QD-bacteria interactions were pre-incubated with 1 mM solutions of $NiCl_2$ (pH 8.5) for 30 min. Unbound QDs were removed by copiously washing the *V. harveyi* cells with PBS, and the samples for optical measurements were prepared by smearing the cells on glass slides coated with poly-L-Lysine.

Fluorescence images of the samples were acquired in an upright optical microscope (Olympus BX 51) equipped with a 100 X oil immersion objective lens, a band pass (510-560 nm) filter for excitation, a dichroic filter that rejects the excitation light, and a band pass (565-640 nm) filter for emission. The source for optical excitation was 510-560 nm light from a 100 W mercury lamp (model: U-LH 100HG). The images *V. harveyi* cells were captured using a CCD camera (Jenoptic, USA) and processed using the software Image-Pro express (Media cybernetics, USA).

4.2. Toxicity of QDs to bacteria

The toxic effect of CdSe/ZnS QDs, with and without photoexcitation for 60 min, to *V. harveyi* cells were examined by estimating the integrities of cell membrane and DNA using SDS PAGE[26] and comet assays. Negative, i.e. without QDs, and positive, i.e. with up to 500 µM cadmium chloride, controls of toxicity were also examined. For SDS assay, *V. harveyi* cells from an overnight culture were washed copiously with sterile PBS and dispensed in 2 mL PBS in sterile quartz cuvettes. After measurement of the initial absorbance, the test solutions were exposed to the above experimental conditions and the absorbencies were recorded at every 5 min for a period of 30 min. The percentage decrease in the absorbencies was compared with the initial reading by plotting absorbencies against time under incubation.

For comet assay, 10^6 *V. harveyi* cells from each experimental group were mixed with 100 µl of 0.5 % low melting point agarose prepared in TAE buffer that contains RNAse (5 g/mL), SDS (0.25 %) and lysozyme (0.5 mg/mL). Bacterial cells impregnated in the agarose suspension were spread over a microscopic comet slide that was pre-coated with a thin layer of agarose (0.5 %). The cells on the slides were lysed at 37 °C for 1 h, by immersing in a lysis solution, which was followed by incubation of the slide in an enzyme solution for 2 h at 37 °C. Subsequently, the slides were equilibrated with 300 mM sodium acetate solution and subjected for electrophoresis at 25 V for 1 h. Following electrophoresis, at first,

the slides were immersed in 1M ethanolic ammonium acetate for 30 min, which was followed by immersing in absolute ethanol for 1 h. Next, the slides were dried at 25 °C and immersed in 70 % ethanol for 30 min. Finally, the slides were dried and stained using a freshly prepared solution of SyBr green nuclear staining dye. The comets of DNA were recorded using an optical microscope (Olympus BX 51) equipped with filters for excitation (470-490 nm) and emission (500 nm dichroic filter and a 520 nm long-pass filter), and a CCD camera. The lengths of the comets formed were measured and processed using the Image Pro express software (Media Cybernetics, USA). Damage to the genetic materials was determined as low (0-10 μm), medium (10-20 μm) or heavy (>20 μm) by classifying the lengths of the comets.

The effect of QDs on survival of *V. harveyi* was estimated by growth rate measurement. Here the *V. harveyi* cells before and after exposure to QDs and $CdCl_2$ were inoculated separately into fresh ZoBell's marine broth (100 mL) and kept at 28 ± 2 °C on a shaker incubator at 120 rpm for 24 h. Aliquots of 1mL of the culture was withdrawn at different time intervals, serially diluted, and spread over the surface of ZoBell's marine agar plates. The plates were incubated at 28 ± 2 °C for 24 h, and colony forming units were counted. The growth rate (μ) of *V. harveyi* was calculated using the equation

$$\mu = \frac{lnNf - lnNi}{Tf - Ti}.$$

Here, Ni and Nf are the number of *V. harveyi* at the beginning (Ti) and end (Tf) of the incubation period.

4.3. Extraction of outer membrane proteins

Outer membrane proteins of *V. harveyi* cells were extracted according to the protocol given in refs. 26 and 27, with minor modifications. Briefly, the cells were washed copiously with sterile saline and re-suspended in PBS supplemented with 5 mM phenylmethylsulfonyl fluoride (PMSF). The cells were burst in an ultrasound sonicator until the cell suspension became translucent. Unbroken cells and cellular debris were removed by centrifugation at 5000 x g for 20 min. The pellet was discarded and the supernatant collected was further centrifuged at 100000 x g in an ultracentrifuge (Beckman Coulter) for 40 min at 4 °C. Again, the supernatant was discarded and the pellet formed was re-suspended in 2 % (w/v) SDS and incubated at room temperature of 25 °C for 1 h, which was followed by centrifugation at 100000 x g for 40 min at 4 °C. The resulting pellet was re-suspended in PBS and stored at -20 °C for further experiments. Outer membrane proteins were analysed by SDS-PAGE with 15 % acrylamide in the separating gel and 5 % acrylamide in the stacking gel. The proteins were visualized by staining with 0.2 % Coomassie brilliant blue G250 in a gel documentation system.

Interaction of CdSe/ZnS QDs with Omps

Outer membrane proteins (Omps) (35 μL) samples were dispensed into sterile microcentrifuge tubes and incubated with CdSe/ZnS QDs (25 nM) for 30 min. Omps-QD conjugates were resolved using polyacrylamide gel electrophoresis as mentioned above. After electrophoresis, the gel was placed over a UV transilluminator (BioRad, USA) for locating the QD fluorescence, and Omps were visualized by staining with 0.2 % Coomassie brilliant blue G250 in an epifluorescent gel documentation system.

4.4. Interaction of QD-bacteria conjugates with animal cell line

Mouse fibroblast L929 cells were cultured up to ~ 50 % confluence in a 25 mL tissue culture flask containing Dulbecco's modified Eagle's medium (DMEM, GIBCO) supplemented with 10 % heat inactivated fetal bovine serum (FBS, GIBCO). The samples were washed copiously with PBS and supplemented individually with 5 mL PBS containing either 1nM CdSe/ZnS QDs or 100 μl *V. harveyi* conjugated with 1nM CdSe/ZnS QDs (QD-bacteria conjugate). The cells were incubated at 37 °C for 2 h in a CO2 (5 %) incubator. Subsequently, the unbound QDs or QD-Vibrio conjugates were removed by copiously washing with PBS. Fluorescent images of the labelled cells were acquired in an inverted optical microscope equipped with a 40 X objective lens, fluorescence filters for QDs, and a CCD camera.

Acknowledgements

AA is thankful to Director, CSIR-NIO Goa and Scientist-in-Charge CSIR-NIO Regional Centre Kochi. AA acknowledge the grant-in-aid for scientific research MOES/ICMAM PD/AOGIA/32/2012 from MoES. Aparna and Esha are thankful to DBT for their M. Tech. fellowship. CJ is a recipient of Women Scientist-A Postdoctoral Fellowship, Department of Science and Technology. VB acknowledges grant-in-aid for scientific research 15H01099 from JSPS.

Notes and references

[1]National Centre for Aquatic Animal Health, Cochin University of Science and Technology, Kochi 682 016, India

[2]Council of Scientific and Industrial Research (CSIR)- National Institute of Oceanography (NIO), Regional Centre Cochin, Kochi 682 018, India

[3]Amity Institute of Virology and Immunology, Amity University, Noida, Uttar Pradesh 201 313 India

[4] Health Research Institute, AIST, 2217-14 Hayashi-Cho, Takamatsu, Kagawa 761-0395, Japan

*Address correspondence to: Abdulaziz Anas (anas@nio.org), Vasudevanpillai Biju (v.biju@aist.go.jp)

1. T. Vu, W. Lam, E. Hatch and D. Lidke, *Cell Tissue Res*, 2015, DOI: 10.1007/s00441-014-2087-2, 1-16.
2. V. Biju, D. Muraleedharan, K. Nakayama, Y. Shinohara, T. Itoh, Y. Baba and M. Ishikawa, *Langmuir*, 2007, **23**, 10254-10261.
3. K. David Wegner and N. Hildebrandt, *Chemical Society Reviews*, 2015, **44**, 4792 - 2834.
4. N. Theilacker, E. E. Roller, K. D. Barbee, M. Franzreb and X. Huang, *Journal of the Royal Society Interface*, 2011, **8**, 1104-1113.
5. A. Anas, T. Okuda, N. Kawashima, K. Nakayama, T. Itoh, M. Ishikawa and V. Biju, *Acs Nano*, 2009, **3**, 2419-2429.
6. C. Chen, J. Peng, H. S. Xia, Q. S. Wu, L. B. Zeng, H. Xu, H. W. Tang, Z. L. Zhang, X. B. Zhu, D. W. Pang and Y. Li, *Nanotechnology*, 2010, **21**, 6.
7. B. Dubertret, P. Skourides, D. J. Norris, V. Noireaux, A. H. Brivanlou and A. Libchaber, *Science*, 2002, **298**, 1759-1762.
8. B. Ballou, B. C. Lagerholm, L. A. Ernst, M. P. Bruchez and A. S. Waggoner, *Bioconjugate Chemistry*, 2004, **15**, 79-86.
9. A. M. Derfus, W. C. W. Chan and S. N. Bhatia, *Advanced Materials*, 2004, **16**, 961 - 964.
10. N. Kawashima, K. Nakayama, K. Itoh, T. Itoh, M. Ishikawa and V. Biju, *Chemistry-a European Journal*, 2010, **16**, 1186-1192.
11. V. Biju, A. Anas, H. Akita, E. S. Shibu, T. Itoh, H. Harashima and M. Ishikawa, *ACS Nano*, 2012, **6**, 3776 - 3788.

12. P. Zrazhevskiy, M. Sena and X. H. Gao, *Chemical Society Reviews*, 2010, **39**, 4326-4354.
13. V. Biju, T. Itoh and M. Ishikawa, *Chemical Society Reviews*, 2010, **39**, 3031-3056.
14. L. Li, X. Qu, J. T. Sun, M. X. Yang, B. F. Song, Q. Q. Shao, X. L. Zhang and W. R. Jin, *Biosens. Bioelectron.*, 2011, **26**, 3688-3691.
15. Y. Zhao, M. Ye, Q. Chao, N. Jia, Y. Ge and H. Shen, *Journal of Agricultural and Food Chemistry*, 2009, **57**, 517 - 524.
16. L. Zhu, S. Ang and W.-T. Liu, *Applied and Environmental Microbiology*, 2004, **70**, 597 - 598.
17. A. Anas, H. Akita, H. Harashima, T. Itoh, M. Ishikawa and V. Biju, *Journal of Physical Chemistry B*, 2008, **112**, 10005-10011.
18. E. S. Shibu, M. Hamada, N. Murase and V. Biju, *Journal of Photochemistry and Photobiology C-Photochemistry Reviews*, 2013, **15**, 53-72.
19. J. A. Kloepfer, R. E. Mielke, M. S. Wong, K. H. Nealson, G. Stucky and J. L. Nadeau, *Applied and Environmental Microbiology*, 2003, **69**, 4205 - 4213.
20. Y. Liu, M. Zhou, D. Luo, L. Wang, Y. Hong, y. Yang and Y. Sha, *Biochemical and Biophysical Research Communications*, 2012, **425**, 769 - 774.
21. V. Biju, T. Itoh, A. Anas, A. Sujith and M. Ishikawa, *Analytical and Bioanalytical Chemistry*, 2008, **391**, 2469-2495.
22. S. Kim, Y. T. Lim, E. G. Soltesz, A. M. De Grand, J. Lee, A. Nakayama, J. A. Parker, T. Mihaljevic, R. G. Laurence, D. M. Dor, L. H. Cohn, M. G. Bawendi and J. V. Frangioni, *Nat. Biotechnol.*, 2004, **22**, 93-97.
23. J. H. K. Preister, P. Stoimenov, R. E. Mielke, S. M. Webb, J. P. D. Zhang, G. Stucky and P. A. Holden, 2589-94., *Environmental Science and Technology*, 2009, **4**, 2589 - 2594.
24. S. Mahendra, H. Zhu, V. L. Colvin and P. J. Alvarez, *Environmental Science and Technology*, 2008, **42**, 9424 - 9430.
25. M. A. Hahn, J. S. Tabb and T. D. Krauss, *Analytical Chemistry*, 2005, **77**, 4861 - 4869.
26. C. N. Lok, C. M. Ho, R. Chen, Q. Y. He, W. Y. Yu, H. Sun, P.-H. Tam, J.-F. Chiu and M. Che, *Journal of Proteome Research*, 2006, **5**.
27. A. A. Belaaouaj, S. K. Kim and D. S. Shapiro, *Science*, 2000, **289**, 1185 - 1187.
28. F. B. Abdallah, H. Kullel and A. Bakhrouf, *Archives of microbiology*, 2009, **191**, 493 - 500.
29. T. A. Kelf, V. K. A. Sreenivasan, J. T. Sun, E. J. Kim, E. M. Goldys and A. V. Zvyagin, *Nanotechnology*, 2010, **21**, 8.
30. M. M. Sharma, Y. I. Chang and T. F. Yen, *Colloids and Surfaces*, 1985, **16**, 193 - 206.
31. Y. E. Collins and G. Stotzky, *Applied and Environmental Microbiology*, 1992, **58**, 1592 - 15600.
32. D. Hühn, K. Kantner, C. Geidel, S. Brandholt, I. De Cock, S. J. H. Soenen, P. Rivera_Gil, J.-M. Montenegro, K. Braeckmans, K. Müllen, G. U. Nienhaus, M. Klapper and W. J. Parak, *ACS Nano*, 2013, **7**, 3253 - 3263.
33. R. Walters, I. L. Mendintz, J. B. Delehanty, M. H. Stewart, K. Susume, A. L. Huston, P. E. Dawson and G. Dawson, *ASN Neuro*, 2015, **7**, 1 - 12.
34. N. P. Singh, R. E. Stephens, H. Singh and H. Lai, *Mutation Research*, 1999, **429**, 159 - 168.
35. A. M. Derfus, W. C. W. Chan and S. N. Bhatia, *Nano Lett.*, 2004, **4**, 11 - 18.
36. P. Jones, S. Sugino, S. Yamamura, F. Lacy, V. Biju, Nanoscale 2013, **5**, 9511 - 9516.
37. S. Yamashita, M. Hamada, S. Nakanishi, H. Saito, Y. Nosaka, S. Wakida, V. Biju, *Angew. Chem. Int. Ed.* 2015, **54**, 3892 - 3896.
38. M. Bottrill and M. Gree, *Chemical Communications*, 2011, **47**, 7039 - 7050.
39. Q. Xiao, S. Huang, W. Su, P. Li and Y. Liu, *Thermochimica Acta*, 2013, **552**, 98 - 105.
40. B. I. Ipe, M. Lehnig and C. M. Niemeyer, *small*, 2005, **1**, 706 - 709.
41. P. Demchick and A. L. Koch, *Journal of Bacteriology*, 1996, **178**, 768 - 773.
42. J. A. Kloepfer, R. E. Mielke and J. L. Nadeau, *Applied and Environmental Microbiology*, 2005, **71**, 2548 - 2557.
43. A. G. White, N. Fu, W. M. Leevy, J.-J. Lee, M. A. Blasco and B. D. Smith, *Bioconjugate Chemistry*, 2010, **21**, 1297-1304.
44. S. K. Chakraborty, J. A. J. Fitzpatrick, J. A. Phillippi, S. Andreko, A. S. Waggoner, M. P. Bruchez and B. Ballou, *Nano Letters*, 2007, **7**, 2618 - 2626.

TOC Graphic

Fluorescence detection of the pathogenic bacteria *Vibrio harveyi* in solutions and animal cells using semiconductor quantum dots

E. Arshad, A. Anas, A. Asok, C. Jasmin, S. S. Pai, I. S. B. Singh, A. Mohandas, V. Biju

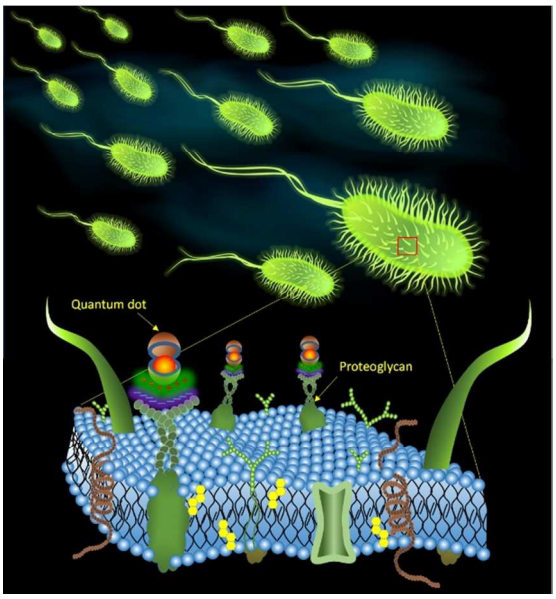

Nanoparticle-based pathogen detection